communications physics

ARTICLE

https://doi.org/10.1038/s42005-022-01090-z OPEN

Exact multistability and dissipative time crystals in interacting fermionic lattices

Hadiseh Alaeian[1] & Berislav Buča[2,3]✉

The existence of multistability in quantum systems beyond the mean-field approximation remains an intensely debated open question. Quantum fluctuations are finite-size corrections to the mean-field as the full exact solution is unobtainable and they usually destroy the multistability present on the mean-field level. Here, by identifying and using exact modulated dynamical symmetries in a driven-dissipative fermionic chain we exactly prove multistability in the presence of quantum fluctuations. Further, unlike common cases in our model, rather than destroying multistability, the quantum fluctuations themselves exhibit multistability, which is absent on the mean-field level for our systems. Moreover, the studied model acquires additional thermodynamic dynamical symmetries that imply persistent periodic oscillations, constituting the first case of a boundary time crystal,to the best of our knowledge, a genuine extended many-body quantum system with the previous cases being only in emergent single- or few-body models. The model can be made into a dissipative time crystal in the limit of large dissipation (i.e. the persistent oscillations are stabilized by the dissipation) making it both a boundary and dissipative time crystal.

[1] Elmore Family School of Electrical and Computer Engineering, Department of Physics and Astronomy, Purdue Quantum Science and Engineering Institute, Purdue University, West Lafayette, IN 47907-2035, USA. [2] Clarendon Laboratory, University of Oxford, Parks Road, Oxford OX1 3PU, UK. [3] Niels Bohr International Academy, Niels Bohr Institute, Copenhagen University, Universitetsparken 5, 2100 Copenhagen, Denmark. ✉email: berislav.buca@physics.ox.ac.uk

Multistability in driven-dissipative models usually means the presence of two possible stationary states of the system that can be distinguished by local observable measurements. Although on the level of the mean-field approximation or for classical systems it can be easily established whether or not it exists[1,2], its actual existence, in particular in low-dimensional strongly interacting systems remains quite controversial with both theoretical and experimental works reporting differing conclusions[3–26]. The existing approaches usually rely on sophisticated theoretical techniques for including perturbations of finite-size corrections to the mean-field or large scale efficient numerical simulations such as t-DMRG[10] or projected entangled pair states (PEPS)[21]. The general lore in the literature is that the lower dimension, the more likely it is that the full quantum fluctuations (finite-system size corrections) will destroy the multistability and restore the generic unique stationary state of the model[27–30]. However, in general, the question remains unsettled in any dimension (see e.g., ref. [21] for an advanced numerical study in two dimensions). Therefore, exact results on this controversial problem are desirable.

There are two recently introduced concepts, dissipative time crystals[31–46], which are systems that have persistent oscillations induced by the dissipation, and boundary time crystals[47–51], which have persistent oscillations in the thermodynamic limit, only (cf. discrete, driven versions of time crystals under dissipation[52–58] and other non-stationary phenomena beyond observables[59–74]). As the oscillations in our model are persistent in the thermodynamic limit, the model can be understood as a boundary time pseudo-crystal, with pseudo- implying that the oscillations amplitude decays with the system size for initial states with low entanglement, similar to long-range order in a pseudo-condensate[75]. Furthermore, as the open system has sustainable oscillations stabilized by very strong dissipation, i.e., quantum Zeno regime, the model is a dissipative time crystal, as well.

Here, we report an exactly solvable model describing a broad class of driven-dissipative and interacting fermionic chains that shows quantum multistablity related to the strong symmetries of the Liouvillian. In general, the strong symmetries are not necessary for the existence of multistability (as degenerate stationary states may emerge in the thermodynamic limit only without a strong symmetry), nor are they sufficient since all of the degenerate stationary states implied by the strong symmetries may have the same expectation values for local observables. More generally, multistability is taken to be an effect not due to any manifest symmetry. However, in our case emergent strong symmetries do guarantee multistability in local observables. In contrast to other potentially bistable models[27], here, rather than being detrimental, quantum fluctuations are essential for the multistability. Further, we show that for certain types of jump operators the Liouvillian has dynamical symmetries that lead to sustainable oscillations in the non-equilibrium long-time behavior of the system, a phenomenon known as dissipative time crystal. Our approach is based on identifying a novel modulated[76] spectrum generating algebra (SGA)[77], which is non-local and fermionic. Since standard dynamical symmetries[31] are extensive and local SGA[78,79] and the SGA here is extensive and semi-local in spin, we call it a semi-local dynamical symmetry[80]. This dynamical symmetry, being fermionic, cannot be relegated to a non-Abelian symmetry, unlike previously known cases based on closed algebras settling the question of whether such operator relations are possible[81]. Later, for sake of simplicity, we specialize the general dissipative-driven fermionic model to a quadratic model and show that these models have an infinite set of emergent (thermodynamic) super-extensive raising operators that we call super-extensive dynamical symmetries. We provide evidence that the total effect of all these operators is that the model displays very slow finite-size decay due to the presence of strong symmetries[82], which guarantee degenerate stationary states (null space of Liouvillian). These have attracted lots of interest recently due to their utility for quantum information storage [83–96]. Moreover, as this behavior is robust to a wide-class of perturbations and occurs in the thermodynamic limit any for generic parameter values, it also constitutes the first example of a boundary time crystal, to the best of our knowledge, in an short-range interacting model. We also derive an analytical lower bound for the decay of such behaviors when the dynamical symmetry is not exact. Finally, we support our theoretical findings using a phase space approach to numerically calculate the Liouvillain spectrum as well as the correlation functions dynamics of the open quantum system dynamics highlighting the emergence of the dissipative time crystalline and the quantum multistabiliy as well as the scaling with the system size.

Results and discussion

The model. Consider the following interacting Kitaev chain model[97],

$$H = -\frac{1}{2}\sum_{i=1}^{N}\left(wc_i^\dagger c_{i+1} + \Delta c_i c_{i+1}\right) + H.c. + \mu\sum_i n_i + V\sum_j (c_j + c_j^\dagger)(c_{j+1} + c_{j+1}^\dagger)(c_{j+2} + c_{j+2}^\dagger)(c_{j+3} + c_{j+3}^\dagger), \quad (1)$$

with $c_j^\dagger$ and c_j being the (Dirac) fermionic creation and annihilation operator, w is the hopping amplitude, Δ is the p-wave pairing correlation, μ is the on-site chemical potential, and V is a novel interacting (beyond-quadratic in general) term we use to model the stronly interaction Majorana fermions, physically originated from electron-electron interactions[98]. The number operators are $n_j = c_j^\dagger c_j$ and the chain is subject to the periodic boundary condition, i.e., $c_{N+1} = c_1$. We note that complex values of coupling coefficients can be physically realized with e.g., constant phase gradients[99] or laser coupling as recently employed in the simulation of a bosonic ladder[100].

This model is commonly mapped onto a spin-1/2 transverse field Ising model at $V = 0$[101]. Note that the model we consider here is not mappable to integrable XYZ spin chains or noninteracting models in contrast to other interesting results[102,103].

As will be apparent shortly, it is convenient to define Majorana fermion operators as,

$$\gamma_{2j-1} = c_j + c_j^\dagger \qquad \gamma_{2j} = i(c_j - c_j^\dagger). \quad (2)$$

These fulfill the following anti-commutation relations,

$$\{\gamma_j, \gamma_m\} = 2\delta_{jm}. \quad (3)$$

Furthermore, here we will study a dissipative case with an incoherent Markovian driving modeled by a Lindblad master equation,

$$\frac{d\rho}{dt} = \hat{\mathcal{L}}[\rho], \quad (4)$$

where $\hat{\mathcal{L}}$ is a quantum Liouvillian of the form

$$\hat{\mathcal{L}}[\rho] = -\mathrm{i}[H,\rho] + \sum_\mu\left(2L_\mu\rho L_\mu^\dagger - \{L_\mu^\dagger L_\mu, \rho\}\right), \quad (5)$$

and the Lindblad jump operators are local Majorana dissipation, as incoherent local single-fermion drive and dissipation of the form $L_{j,1} = \sqrt{\Gamma}(c_j^\dagger + c_j) = \sqrt{\Gamma}\gamma_{2j-1}$, $j = 1, \ldots N$. The quadratic version of this model ($V = 0$) has been previously studied for its topological properties[104]. We will also consider a special type of dissipative pairing as $L_{j,2} = \sqrt{\varepsilon}(c_j + c_j^\dagger)(c_{j+1} + c_{j+1}^\dagger) = \sqrt{\varepsilon}\gamma_{2j-1}\gamma_{2j+1}$ which can be engineered with Pauli blocking[105].

It is useful to define a vector space of operators with the standard Hilbert-Schmidt inner product, as $\langle\langle A|B\rangle\rangle = \mathrm{tr}(A^\dagger B)$, with a corresponding norm that we will use.

In order to solve the dynamics of $\rho(t)$ it is useful to diagonalize $\hat{\mathcal{L}}$. Define λ_k to be the eigenvalues of $\hat{\mathcal{L}}$ and ρ_k, σ_k to be the corresponding right and left eigenoperators, respectively,

$$\hat{\mathcal{L}}[\rho_k] = \lambda_k \rho_k,\ \hat{\mathcal{L}}^\dagger[\sigma_k] = \lambda_k^* \sigma_k, \\ \langle\langle \sigma_k|\rho_{k'}\rangle\rangle = \delta_{k,k'}. \tag{6}$$

Due to the semi-group properties of the Lindblad master equation all the eigenoperators are either stable or decaying, i.e., $\mathrm{Re}(\lambda_k) \le 0$. Further, they always appear in complex conjugate pairs as $\{\lambda_k, \lambda_k^*\}$. Since the jump operators L_μ are Hermitian in our model, the Lindblad equation is unital, and the identity matrix is always a non-equilibrium steady state (NESS), i.e., $\rho_0 = \mathbb{1}$.

We are interested in the dynamics of observables $O(t)$ when we initalize the system in $\rho(0)$. Formally, the solution can be written as

$$\langle O(t)\rangle = \sum_k e^{t\lambda_k} \langle\langle O|\rho_k\rangle\rangle \langle\langle \sigma_k|\rho(0)\rangle\rangle. \tag{7}$$

Purely imaginary eigenvalues are therefore necessary but not sufficient for persistent oscillations in physical observables due to possibly vanishing overlap of local observables with right eigenoperator, or the zero overlap of the initial state with left eigenoperators, or the presence of dense and incommensurate purely imaginary eigevalues λ_k in the Liouvillian spectrum.

Emergent dynamical symmetries in the thermodynamic limit. The origin of dynamical symmetries can be understood by studying the quadratic version of the model in (1) in the non-interacting limit, i.e., $H_0 = H(V=0)$. The model is then the standard Kitaev Hamiltonian that in the thermodynamic limit can be diagonalized with a Fourier transform followed by a Bogoliubov transformation. We obtain (up to an irrelevant shift),

$$H_0 = \sum_k E_k\, d^\dagger(k) d(k), \tag{8}$$

with the lowering operators of,

$$d(k) = u_k c(k) + v_k c^\dagger(-k), \\ c(k) = \frac{e^{-\mathrm{i}\frac{\pi}{4}}}{\sqrt{N}} \sum_{j=1}^{N} e^{-\mathrm{i}kj} c_j. \tag{9}$$

Here, $c(k)$ is the Fourier transform of the fermion annihilation operator at momentum k and $d(k)$ is its Bogoliubov transformation where the (not-normalized) coefficients are defined as

$$u_k = -\frac{\mathrm{i}\Delta \sin(k)\sqrt{E_k - w\cos(k) - \mu}}{\sqrt{2}\left|\Delta \sin(k)\right|\sqrt{E_k}}, \\ v_k = \frac{\mathrm{i}(E_k + w\cos(k) + \mu)}{\Delta \sin(k)} u_k, \tag{10}$$

and the energy is,

$$E_k = \sqrt{\left|\Delta \sin(k)\right|^2 + (w\cos(k) + \mu)^2}. \tag{11}$$

The momentum is restricted to the first Brillouin zone $k = \frac{2\pi}{N} m$, $m = -\frac{N}{2} + 1, \ldots, \frac{N}{2} - 1, \frac{N}{2}$.

If for some κ, $u_\kappa = -v_\kappa$, we have up to a multiplicative constant,

$$d_\kappa = \sum_{j=1}^{N} e^{-\mathrm{i}\kappa j} \gamma_{2j}. \tag{12}$$

Solving $u_k = -v_k$ using (10) for purely imaginary Δ gives $\kappa = \cos^{-1}(-\frac{\mu}{w})$, which is a real momentum for $|\mu| < |w|$, coinciding with the topological phase of the Kitaev chain. Using (3) it is clear that even Majorana fermions γ_{2j} commute with any product of an even number of odd Majorana fermions γ_{2j-1}. That means the interaction term of the Hamiltonian in (1) commutes with d_κ from which it directly follows that,

$$[H, d_\kappa] = -E_\kappa d_\kappa, \tag{13}$$

where $E_\kappa = \left|\Delta\sqrt{1 - \frac{\mu^2}{w^2}}\right|$.

Thus d_κ is a modulated fermionic dynamical symmetry of the model. They are essentially similar to Goldstone modes, except they exist at finite frequency and momentum. The dynamical symmetry implies that observables with non-zero overlap with it can persistently oscillate at frequency E_κ[81]. Note that there are special values of parameters for which the dynamical symmetries exist for finite systems, e.g., for $\mu = 0$, $\kappa = \pi/2$ is always a solution for $\mathrm{mod}(N, 4) = 0$. For more general μ, w (with $|\mu| < |w|$); however, the dynamical symmetries exist only in the thermodynamic limit as for finite systems there is no solution for κ for general μ, w. In other words, these dynamical symmetries are emergent for systems that are large enough to have a continuum of momenta k in the 1st B.Z. Hence, they are thermodynamically emergent symmetries.

Now consider the case $\Gamma = 0$. Since the jump operators $L_{j,2}$ are as sums of products of odd Majorana fermions one has $[L_{j,2}, d_\kappa] = 0$. Therefore, $S := d_\kappa$ is an emergent *strong* dynamical symmetry of the open quantum system with dissipators $L_{j,2}$ in the thermodynamic limit[31,106,107], which implies that operators $S^n \rho_\infty (S^\dagger)^m$ are eigenoperators of $\hat{\mathcal{L}}$ with purely imaginary eigenvalues $\mathrm{i}(n-m) E_\kappa$. Here, $n, m = 0, \pm 1$ as $S^2 = \mathbb{1}$. Note that S is local in the fermion basis in the sense of being a sum of local densities.

Here, the eigenstate dephasing[108] is not possible because the purely imaginary eigenspectrum is equally spaced. In order to qualify as a boundary time crystal the system must, in addition to the previous conditions, have persistent oscillations in local observables[47]. This is the case because S is local and has non-zero overlap with local observables meaning that the expectation values of a local observable (by (7)),

$$\lim_{t\to\infty} \langle O(t)\rangle = \mathrm{tr}[O \sum_{n,m} e^{\mathrm{i}(n-m)E_\kappa} c_{n,m} S^n \rho_\infty (S^\dagger)^m], \tag{14}$$

will be finite and persistently time-periodic in the thermodynamic limit. This is clearest when considering the example $O = \gamma_{2j}$ with the asymptotic state $\rho(t) = \mathbb{1} + e^{\mathrm{i}E_\kappa t} S + e^{-\mathrm{i}E_\kappa t} S^\dagger$.

This therefore constitutes, an exact example of a boundary time crystal in an extended many-body system with local interactions. Besides, we conjecture that the model is a dissipative time crystal as well (persistent oscillations induced by dissipation) because the closed model likely has oscillations that dephase due to the multitude of incommensurate eigenvalues[108]. We will discuss robustness of the boundary time crystal state in the next section.

Semi-local dynamical symmetries and stability of the dynamics. We will now consider the case when $\Gamma \neq 0$ and in order to simplify the following discussion we will assume without loss of generality that the parameters of the model are such that the dynamical symmetry exists for some finite values of N, e.g., at $\mu = 0$ as discussed in the previous subsection.

Let us define $m_j = \frac{1}{2}\mathbb{1} - n_j$ and the parity operator $P_{j,k} = \prod_{q=j}^{k} m_q$. We now note some useful identities. The Hamiltonian is parity-symmetric, i.e., $[H, P_{1,N}] = 0$, and the Lindblad jump operators are parity-antisymmetric, i.e., $\{L_{\mu,1}, P_{1,N}\} = 0$ and furthermore satisfy $\{L_{\mu,1}, d_\kappa\} = 0$. From this it follows directly that $[H, P_{1,N} d_\kappa] = -E_\kappa P_{1,N} d_\kappa$ and $[L_{\mu,1}, P_{1,N} d_\kappa] = 0$ hence, $A' = P_{1,N} d_\kappa$ is a non-local strong spectrum generating algebra.

Remark 1: As a side note we will show that this operator leads to a semi-local dynamics symmetry when mapped to the spin systems.

Here, for reasons that will become apparent, we consider the standard Wigner-Jordan mapping[109],

$$\begin{aligned} \tilde{P}_{j,k} &= \prod_{x=j}^{k} \sigma_x^z, \\ c_j &= \tilde{P}_{1,j-1}\sigma_j^-. \end{aligned} \tag{15}$$

Following the mapping in (15), operator A' gets transformed to a semi-local dynamical symmetry in the spin basis, i.e., its densities commute only with operators on one side of the chain with the following form,

$$\tilde{A}' = \sum_{j=1}^{N} \exp(\mathrm{i}\frac{\pi}{2}j)\sigma_j^x \tilde{P}_{j+1,N}. \tag{16}$$

Such semi-local symmetry operators have been studied recently in the context of generalized hydrodynamic corrections in quadratic and integrable models where their existence was associated with the topological nature of the models[80]. Topology likely plays a role in our model as it is intimately related to the Kitaev chain. These new kinds of dynamical symmetries should be distinguished from both local extensive[78,110–112] and strictly local ones[113–115]. We emphasize, that in the model studied here there is no obvious transformation that would allow mapping this semi-local dynamical symmetry into a semi-local non-Abelian symmetry while preserving the spatial locality of H.

The operators A' and $(A')^\dagger$ satisfy fermionic anti-commutation relations $\{A', (A')^\dagger\} = \mathbb{1}$ and they are nilpotent $(A')^2 = 0$.

The existence of A' immediately implies the existence of a super-extensive (quadratic) charge $Q = (A')^\dagger A'$ for which it can be easily shown that $\mathrm{tr}(Q^2)/2^N \propto N^2$ by observing that the expression has only finite trace for those term in the doubled sum when local densities are on the same site. For example, for $\mu = 0$, in the Majorana basis it may be written as,

$$Q = \mathrm{i}\left(\sum_{j=1}^{N} \mathrm{i}^{j-1}\gamma_{2j}\right)\left(\sum_{j=1}^{N/2} (-1)^j \gamma_{4j}\right). \tag{17}$$

This Hermitian operator defines a symmetry $S = e^{\mathrm{i}Q}$ as $[H, S] = 0$. We remark that for the closed system ($\Gamma = \epsilon = 0$), the existence of Q and its growth with system size immediately implies that the memory of the initial state decays as $1/N^2$ in local observables O with $\mathrm{tr}(QO) \neq 0$ as quantified by e.g., infinite temperature auto-correlation functions $\langle O(t)O \rangle$ via the Mazur bound[116].

For the open system, S is a strong symmetry[82,117], which in turn implies that the non-equilibrium stationary state $\lambda_0 = 0$ is degenerate. There, $\rho_0' = \mathbf{1} - (A'(A')^\dagger)$ is the other eigenoperator of the Liouvillian null space for $\lambda_0 = 0$ where we define $\mathbf{1} := \mathbb{1}/(2^N tr[(A'(A')^\dagger)])$, in order for it to be Hilbert-Schmidt orthogonal to the left null space eigenmode $\omega_0 = \mathbb{1}$, i.e., $tr(\rho_0') = 0$. It is worth reminding that due to unitality of the Liouvillian, one NESS is always $\rho_0 = 1/2^N \mathbb{1}$.

Furthermore, based on the properties of A', $\rho_1 = (A')^\dagger$, $\rho_{-1} = A'$ are the bi-orthogonal eigenmodes corresponding to the purely imaginary eigenvalues of $\lambda_{\pm 1} = \mathrm{i}E_\kappa$. Due to unitality the left and right eigenmodes are each others conjugate transposes, i.e., $\sigma_{\mp 1} = \mathcal{N}(\rho_{\pm 1})^\dagger$ up to a normalization constant $\mathcal{N}$.

It is obvious that the presence of purely imaginary eigenvalues is not visible in any local observable O because A' is non-local as it does not contain any local terms hence, $\rho_{\pm 1}$ do not have Hilbert-Schmidt overlap with such observables.

The multistability situation is different however, as ρ_0' has a non-zero overlap with a local observable O (without loss of generality $tr(O) = 0$). In order to estimate its multistability, we first note that a general stationary state must be density matrix and hence a convex combination of the two stationary states $\rho_\infty = \rho_0 = \rho_0 + c\rho_0'$ such that ρ_∞ is positive semi-definite.

Because $||\rho_0||^2 = 1/2^N$, $||\rho_0'||^2 \propto N^2/2^N$ and the eigenvalues of ρ_0' sum into 0 by construction, $c \propto 1/N$. However, since for local observables $\mathrm{tr}(O\rho_0') \propto N^0$ we have for the expectation values,

$$\langle O(t \to \infty) \rangle \propto \langle \langle O | c\rho_0' \rangle \rangle \propto 1/N, \tag{18}$$

which gives a lower bound on the $|\langle O(t \to \infty) \rangle|$. We note that this is only a lower bound because many eigenvalues have vanishing real part in the limit of $N \to \infty$ and hence the actual expectation values can decay slower with N. Thus the model is bistable only for the finite-sized chains where quantum fluctuations are important. This is unlike typical mean-field multistability scenarios occurring in the thermodynamic limit (i.e., $N \to \infty$) where quantum fluctuations do not play a role.

Expanding for small $\varepsilon = O(1/N)$ around $k = \kappa \pm \varepsilon$ we have $[L_\mu, P_{1,N} d_{\kappa \pm \varepsilon}] = \mathcal{O}(\varepsilon)$ (by Taylor series expansion) and, likewise, $[H, d_{\kappa \pm \varepsilon}] = -E_\kappa d_\kappa + O(\varepsilon)$. As $\varepsilon \propto 1/N$, this implies that the dissipative gap (the real part of the eigenvalues of the Liouvillian) closes as $\propto 1/N$ into the same purely imaginary eigenvalues. They are hence metastable[118–120]. We will confirm this in the next section with a concrete example. The closing of the Liouvillian gap is associated with an algebraic temporal relaxation of the dynamics, but as we will see in the next section, it can also lead to larger quantum fluctuations (i.e., slower decay of multistability with N). Therefore, these additional dynamical symmetry lead to a different behavior than the standard power-law decay of multistability and oscillations that are usually studied for Liouvillian gaps closing[121–123].

It is important to note that, even though $A_\kappa^2 = 0$, $A_{\kappa+\varepsilon} A_\kappa \neq 0$ and thus these operators do have overlap with local operators (this follows from $P_{1,N}^2 = \mathbb{1}$), leading to boundary *pseudo*-time crystal behavior in local observables as will be shown in the numerical results subsection.

The dynamical symmetries are responsible for both the boundary (pseudo-)crystal and the multistability. As long as the dynamical symmetries we discovered are present these phenomena will be as well. The semi-local dynamical symmetries are completely non-perturbatively stable to all perturbations that are odd in the Majorana fermions i.e., $D_x = \sum_j x_j^{(1)} \gamma_{2j-1} + x_{j,k}^{(2)} \gamma_{2j-1}\gamma_{2k-1} \cdots$ for arbitrary parameter set x. Namely, lets introduce an arbitrary such perturbation $H \to H + D_x$, $L_{k,\mu} \to L_{k,\mu} + D_{k,y}$. We will still have $[H, A'] = E_k \kappa A'$ and $[L_{k,\mu}, A'] = [L_{k,\mu}^\dagger, A'] = 0$ and A' remains a strong dynamical symmetry. What if the perturbation W is even in the Majorana fermions i.e., $H \to H + sW$, $L_{k,\mu} \to L_{k,\mu} + sW$? In that case the purely imaginary are stable at least to the second order in the small parameter s according to the results of ref. [106]. Hence, an degree of sub-leading stability remains.

Moreover, according to the results of ref. [106] if we can engineer ϵ to be large a quantum Zeno dynamics will emerge. More specifically, the purely imaginary eigenvalues will be stable up to corrections $1/\epsilon^2$ that we can engineer to be small. In other words, the dissipation will stabilize the oscillations to any perturbations. This renders the system a *dissipative* time crystal in the sense of dissipation inducing persistent oscillations in the our many-body system[31].

Numerical results. In this section, for sake of simplicity, we will focus on the quadratic model, noting that the general conclusion, according to the discussion in the previous sections, holds for the interacting models, as well.

Besides, as the open system with $L_{\mu,2}$ jump operators leads to an exact time-periodic behavior as discussed here we merely focus on $L_{\mu,1}$ dissipators to show the finite-size scaling.

To check the existence of the pure imaginary eigenvalues λ_k and find the multiplicity of the null space, we employ the third quantization method for calculating the Liouvillian spectrum for N-fermion chains where $\mathrm{mod}\,(N,4)=0$ subject to the periodic boundary conditions, as described in the model subsection. As the conserved dynamics is quadratic and the jump operators are linear in fermionic basis the Liouville super-operator ($\mathcal{L}$) can be diagonalized in terms of $2N$ normal master modes acting on the Fock states of density operators[124]. The eigenvalues of the super-operator (λ_k) can be obtained directly from the spectrum of the shape matrix, aka rapidities (β_i) as

$$\lambda_{\overrightarrow{\nu}} = -2\sum_{i=1}^{2N}\beta_i\nu_i, \tag{19}$$

where $\overrightarrow{\nu}$ is a $2N$-long binary string. An alternative approach, also finding a closing spectral gap in related models, can be found in[125].

The whole Liouvillian spectrum can be exactly calculated by considering all $\overrightarrow{\nu}$ within $(1, 4^N)$. Due to the linear growth of the shape matrix with N, in opposed to an exponential one, one can obtain detailed information about $\mathcal{L}$ without being limited to small N chains hence, an equal treatment of the finite-sized systems and larger one approaching the thermodynamic limit (cf. the methods section further details).

Figure 1a–c shows the Liouvillian spectrum (λ_k) of noninteracting Kitaev model in (1) for $\mu=0, w=1, \Delta=i$ at different chain lengths of $\mathrm{N}=4$, 12, and 100, respectively. For cases (b) and (c) the spetrum is zoomed in close to the imaginary axis to highlight the slowly decaying eigenvalues. The red dots show the pure imaginary eigenvalues at $\lambda_{\pm}=\pm 2i$, and the green dot corresponds to the degenerate NESS at $\lambda_0=0$.

To examine the multistability and the long-time behavior of the system we study the two-point correlations and their time evolution. As the whole dynamics, including both the conservative and the dissipative part, is quadratic the state is Gaussian hence its first and second moments (two-point correlation functions) are sufficient to describe the system, fully. Using the Heisenberg picture we can derive the following equations of motion for the two-point correlation functions

$$\begin{aligned}\frac{d}{dt}\langle c_m c_n\rangle =& \mathrm{i}\Big(w\langle c_{m+1}c_n\rangle + w\langle c_m c_{n+1}\rangle + w^*\langle c_{m-1}c_n\rangle + w^*\langle c_m c_{n-1}\rangle \\ &+ 2\mu\langle c_m c_n\rangle - \Delta^*\langle c_n c^\dagger_{m+1}\rangle + \Delta^*\langle c_n c^\dagger_{m-1}\rangle\Big) \\ &+ \mathrm{i}\Big(\Delta^*\langle c_m c^\dagger_{n+1}\rangle - \Delta^*\langle c_m c^\dagger_{n-1}\rangle\Big) \\ &+ 2\sum_k \gamma_k\Big(\big(\langle c_k\rangle + \langle c^\dagger_k\rangle\big)\big(\langle c_m\rangle\delta_{nk} - \langle c_n\rangle\delta_{mk}\big)\Big),\end{aligned} \tag{20}$$

$$\begin{aligned}\frac{d}{dt}\langle c^\dagger_m c_n\rangle =& \mathrm{i}\Big(-w\langle c^\dagger_{m-1}c_n\rangle + w\langle c^\dagger_m c_{n+1}\rangle - w^*\langle c^\dagger_{m+1}c_n\rangle + w^*\langle c^\dagger_m c_{n-1}\rangle \\ &+ \Delta\langle c_{m-1}c_n\rangle - \Delta\langle c_{m+1}c_n\rangle\Big) + \mathrm{i}\Big(-\Delta^*\langle c^\dagger_m c^\dagger_{n-1}\rangle + \Delta^*\langle c^\dagger_{n+1}c^\dagger_m\rangle\Big) \\ &+ 2\sum_k \gamma_k\Big(\big(\langle c_n\rangle\delta_{mk} - \langle c^\dagger_m\rangle\delta_{nk}\big)\big(\langle c_k\rangle + \langle c^\dagger_k\rangle\big)\Big).\end{aligned} \tag{21}$$

As can be seen, correlations make a closed set of coupled nonlinear equations that can be numerically solved knowing the initial states.

The time evolution of a local two-point correlation ($\langle\hat{c}_1\hat{c}_2\rangle$) of such chains is presented in Fig. 2 showcasing the emergence of both non-stationary steady states, aka dissipative time crystal, and the multistability, manifested by two distinct values at long-time limit. Since the long-time solutions in the bistable region depend on the initial state (cf. (7)), the equations of motion as in (20) and (21) are evolved for randomized initial states, two of them shown as red and blue lines in each panel.

To examine the scaling of the local observable with the system size (N) in Fig. 3 we plot the long-time value of $|\langle\hat{c}_1\hat{c}_2\rangle|$ as a function of the chain length.

The dots show the results of the numerical calculations when the initial correlations are chosen to be $\langle\hat{c}_n\hat{c}_m\rangle = 1+\mathrm{i}$ and $\langle\hat{c}_n\hat{c}^\dagger_n\rangle = 0$, i.e., having one particle on each site. As can be seen the correlation for smaller system sizes follows a power-law behavior decaying as N^{-1} (red line in Fig. 3) consistent with the lower bound prediction of the semi-local dynamical symmetries and stability of the dynamics subsection. For longer chains, i.e., larger N, more semi-local dynamical symmetries (semi-local finite-frequency Goldstone modes) start emerging and the decay with N slows down, consistent with the results of the emergent dynamical symmetric in the thermodynamic limit subsection. More specifically,

$$\langle O(t\to\infty)\rangle = \sum_k e^{t(\mathrm{i}\omega_k + \mathcal{O}(1/N))}\langle\langle O|\rho_k\rangle\rangle\langle\langle\sigma_k|\rho(0)\rangle\rangle. \tag{22}$$

with $\omega_k \in \mathbb{R}$ and the complex decay rate goes down as $\mathcal{O}(1/N)$). This implies both multistability and the persistent oscillations.

Conclusions

In this paper we have shown that for large classes of driven strongly interacting models there exist spectrum generating algebras that are semi-local in the spin basis, which we therefore named semi-local dynamical symmetries. They generically are manifest in the thermodynamic limit only. Physically, they correspond to particle excitations that are invisible to the interaction. They also imply non-local (quadratic) conservation laws, which are promoted to strong symmetries when the system is subjected to pair dephasing. Being quadratic, these operators directly imply memory of the initial condition, i.e., degenerate stationary states and multistability that decays with system size. This means that, unlike previously studied cases of multistability, here the multistability is present in the quantum fluctuations and in the finite-size systems (beyond mean-field) rather than being destroyed by them. Our work implies that genuine (fully exact) multistability for quantum many-body systems requires emergent symmetry structure in the thermodynamic limit, even though a manifest one is not necessarily present for the finite-size system.

The system in the thermodynamic limit obtains further emergent dynamical symmetries, which are finite-frequency and

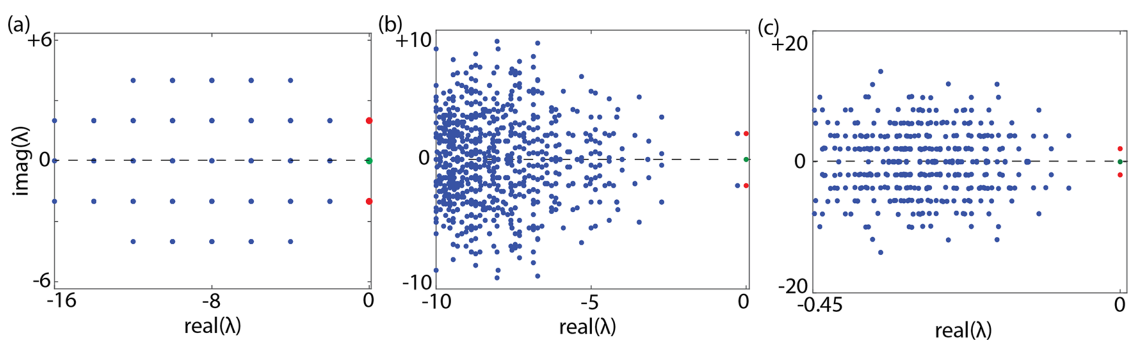

Fig. 1 Liouvillian gap closure and the signature of the non-stationary phase. Liouvillian spectrum of noninteracting Kitaev chain for different chain length **a** $\mathrm{N}=4$, **b** $\mathrm{N}=12$, and **c** $\mathrm{N}=100$ subject to periodic boundary conditions. In all cases the chemical potential, hopping amplitude, and pairing potential are $\mu=0, w=1, \Delta=i$, respectively. The red and green dots show the pure imaginary and zero eigenvalues, respectively.

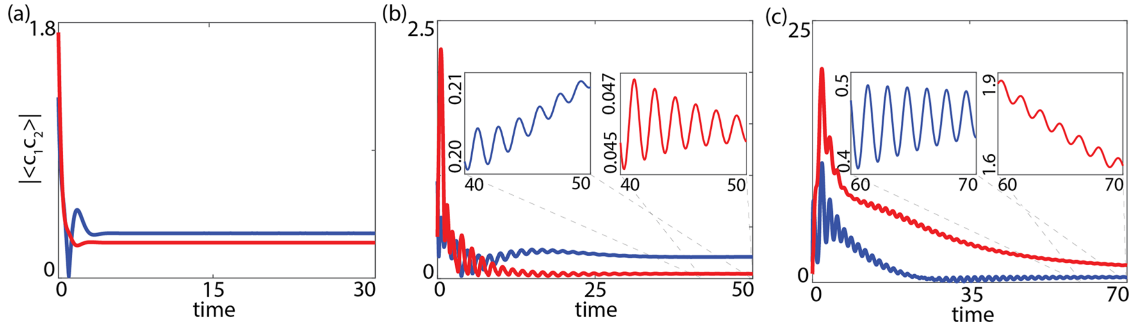

Fig. 2 Multistability and non-stationary behavior vs. the system size. Time evolution of the first and the second site correlation ($|\langle\hat{c}_1\hat{c}_2\rangle|$) showcasing the multistability for two randomized initial states and the oscillatory behavior for various chain length of **a** N = 4, **b** N = 12, and **c** N = 100 subject to the periodic boundary condition. Blue and red lines correspond to two different randomized initial conditions.

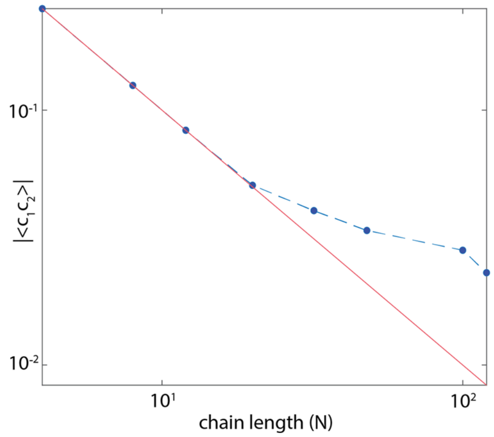

Fig. 3 Observable scaling with the system size. Local observable scaling vs. the chain length N when the initial correlation in all cases is the same as two-site correlation of $\langle\hat{c}_n\hat{c}_m\rangle = 1 + i$ and initial occupation of $\langle\hat{c}_n^\dagger\hat{c}_n\rangle = 1$. The dots are the results of the moments equations of motion integration, the dashed line is guide to the eye, and the red line is N^{-1} scaling for comparison.

finite-momentum quasi-particles dressing the original dynamical symmetry excitations. Therefore, we call these emergent dynamical symmetries semi-local finite-frequency and finite-momentum Goldstone modes. For the dissipative system they imply strong symmetries. These Goldstone modes imply that, as we approach the thermodynamic limit, decay times of oscillations in the local observables diverge, but their amplitude goes to zero at least for initial states that have low-enough entanglement. Hence the system is a boundary time time crystal according to the thermodynamic requirements of ref. [47]. However, the oscillations are clean and periodic both for the isolated (closed $L_\mu = 0$) and dissipative system, therefore our system is not a dissipative time pseudo-time crystal in the sense of the dissipative time crystals introduced in ref. [31], which would imply that dissipation is the one inducing periodic oscillations absent for the isolated system.

To the best of our knowledge, this is the first exact and fully non-perturbative result on the long-debated problem of multistability and multistability in driven-dissipative many-body quantum systems. Although we studied pairing fermionic models, the approach of thermodynamically emergent dynamical symmetries implying quasi-particles that are invisible to certain kinds of interactions is general and can be applied to both bosonic and spin systems. Our work provides an approach for proving presence of multistability in more general and widely studied quantum optical setups.

In future works, we plan to apply our approach to many-body spin and bosonic systems where multistability and persistent oscillations have been experimentally observed in the thermodynamic limit. Exploring the underlying connection between emergent collective behaviors and topology in such systems with quantum synchronization[106,126–128] are other interesting directions of the future studies.

Methods

Shape matrix, rapidities, and Liouvillian spectrum. As described in ref. [124] the two parts of the super-operator, i.e., the conserved dynamics $\hat{\mathcal{L}}_H$ and the non-unitary parts $\hat{\mathcal{L}}_D$ has the following forms

$$\mathcal{L}_H = -i4\sum_{j,k}\hat{c}_j^\dagger H_{jk}\hat{c}_k, \tag{23}$$

and

$$\mathcal{L}_D^+ = 2\sum_{j,k=1}^{2N}\sum_{\mu=1}^{N} l_{\mu j}l_{\mu k}^*\left(2\hat{c}_j^\dagger\hat{c}_k^\dagger - \hat{c}_j^\dagger\hat{c}_k - \hat{c}_k^\dagger\hat{c}_j\right), \tag{24}$$

where $\hat{c}_i, \hat{c}_i^\dagger$ are the super-operator (a-fermion) annihilation and creation operators in the operator Fock space, respectively. Here, we focus on the $\mathcal{K}^+$, i.e., the even sup-space, only.

We define the $4N \times 1$-vector of a-fermionic operators as

$$\hat{\mathbf{C}} = \begin{pmatrix} \hat{c}_1 \\ \cdots \\ \hat{c}_{2N} \\ \hat{c}_1^\dagger \\ \cdots \\ \hat{c}_{2N}^\dagger \end{pmatrix}. \tag{25}$$

With this definition we can write the Liouville super-operator $\hat{\mathcal{L}}^+ = \hat{\mathcal{L}}_H + \hat{\mathcal{L}}_D^+$ as

$$\hat{\mathcal{L}}^+ = \hat{\mathbf{C}}^\dagger \mathbf{L}^+ \hat{\mathbf{C}} = \hat{\mathbf{C}}^\dagger \begin{pmatrix} \mathbf{L}_{11} & \mathbf{L}_{12} \\ \mathbf{0} & \mathbf{L}_{22} \end{pmatrix} \hat{\mathbf{C}}, \tag{26}$$

To write the non-unitary parts easier, we define a matrix with entries $M_{jk} = \sum_{\mu=1}^{N} l_{\mu j}l_{\mu k}^*$ hence, $\mathbf{M} = \mathbf{M}^\dagger$ is a Hermitian matrix.

Using these definitions we have

$$\begin{aligned} \mathbf{L}_{11}^{jk} &= -i2H_{jk} - M_{jk} - M_{kj} = -i2H_{jk} - M_{jk} - M'_{jk}, \\ \mathbf{L}_{12}^{jk} &= 4M_{jk}, \\ \mathbf{L}_{22}^{jk} &= i2H_{kj} + M_{kj} + M_{jk} = -i2H_{jk} + M'_{jk} + M_{jk}. \end{aligned} \tag{27}$$

Considering the antisymmetric properties of $\mathbf{H}$, it becomes apparent that $\mathbf{L}_{11} = -\mathbf{L}_{22}^\dagger$. Therefore, we have

$$\hat{\mathcal{L}}^+ = \hat{\mathbf{C}}^\dagger \begin{pmatrix} -\mathbf{L}_{22}^\dagger & \mathbf{L}_{12} \\ \mathbf{0} & \mathbf{L}_{22} \end{pmatrix} \hat{\mathbf{C}}. \tag{28}$$

The shape matrix A defined in[124] is simply a rotation of this matrix hence, the eigenvalues of A and $\mathbf{L}^+$ are the same. If $\eta_i, i \in \{1, 2, \cdots, 2N\}$ are the eigenvalues of $\mathbf{L}_{22}$ then the eigenvalues of $\mathbf{L}^+$ appear in pairs as $(\eta_i, -\eta_i^*)$. Also from the form of $\mathbf{L}_{22}$ it is clear that the eigenvalues appear in complex conjugate pairs as $(\gamma_i, \gamma_i^*), i \in \{1, 2, \cdots, N\}$. Finally, one can conclude that the spectrum of the shape matrix $\mathbf{A}$ appear in quadruple of $(\xi, \xi^*, -\xi, -\xi^*)$. The rapidities are defined as the subset of the eigenvalues with positive real parts from which the full spectrum of $\mathcal{L}^+$ can be obtained using (19). From this spectrum it becomes evident if there are any kernels, corresponding to multistability, or pure imaginary eigenvalues, corresponding to a non-stationary NESS.

Dispersion of a chain with periodic boundary conditions. Let's consider an N-long chain with periodic boundary conditions (PBC), i.e., $c_{m+N} = c_m$. One can use the following Fourier transformation to find the spectral form

$$\tilde{c}(k) = \frac{1}{\sqrt{N}} \sum_m e^{-imk} c_m \,,\; c_m = \frac{1}{\sqrt{N}} \sum_k e^{imk} \tilde{c}(k). \tag{29}$$

It is straightforward to see that the anti-commutator relations of the Fourier series has the following form

$$\{\tilde{c}(k), \tilde{c}(k')\} = 0 \,,\; \{\tilde{c}(k), \tilde{c}^\dagger(k')\} = \delta_{mn}\delta(k-k'). \tag{30}$$

Replacing each term by its Fourier transform, we get the following spectral form

$$\tilde{H}(k) = \sum_k -2|w|\cos(k+\phi_w)\tilde{c}^\dagger(k)\tilde{c}(k) - \frac{\mu}{2}\left(\tilde{c}^\dagger(k)\tilde{c}(k) - \tilde{c}(k)\tilde{c}^\dagger(k)\right) \tag{31}$$

$$+\Delta e^{-ik}\tilde{c}(k)\tilde{c}(-k) + \Delta^* e^{-ik}\tilde{c}^\dagger(k)\tilde{c}^\dagger(-k) \tag{32}$$

$$= \left(\tilde{c}^\dagger(k)\; \tilde{c}(-k)\right)\begin{pmatrix} -|w|\cos(k+\phi_w) - \frac{\mu}{2} & i\Delta^*\sin k \\ -i\Delta\sin k & |w|\cos(-k+\phi_w) + \frac{\mu}{2}\end{pmatrix}\begin{pmatrix}\tilde{c}(k) \\ \tilde{c}^\dagger(-k)\end{pmatrix}. \tag{33}$$

The choice of this spinor is useful since we can readily write the Fourier transform of Majorana fermions as a direct rotation

$$\begin{pmatrix}\tilde{w}_o(k) \\ \tilde{w}_e(k)\end{pmatrix} = \begin{pmatrix} 1 & 1 \\ i & -i\end{pmatrix}\begin{pmatrix}\tilde{c}(k) \\ \tilde{c}^\dagger(-k)\end{pmatrix}, \tag{34}$$

where the o, e-superscripts refer to the odd and even Majorana fermions.

Substituting this back into the spectral Hamiltonian we can re-write it in terms of the Majorana fermions as

$$H_w = \frac{1}{2}\begin{pmatrix} |w|\sin\phi_w \sin k + \mathrm{Im}(\Delta)\sin k & i\left(|w|\cos\phi_w\cos k + \frac{\mu}{2}\right) - \mathrm{Re}(\Delta)\sin k \\ -i\left(|w|\cos\phi_w\cos k + \frac{\mu}{2}\right) - \mathrm{Re}(\Delta)\sin k & |w|\sin\phi_w\sin k - \mathrm{Im}(\Delta)\sin k\end{pmatrix} \tag{35}$$

If the jump operators are identical for all fermionic sites as $L_j = \sqrt{g}\left(c_j + \delta c_j^\dagger\right)$, then $\mathbf{M}$ will read as follows

$$\mathbf{M} = \frac{g}{4}\begin{pmatrix} |1+\delta|^2 & i\left(1-|\delta|^2\right) - 2\mathrm{Im}(\delta) \\ -i\left(1-|\delta|^2\right) - 2\mathrm{Im}(\delta) & |1-\delta|^2\end{pmatrix} \tag{36}$$

Finally, we can use (27) to determine the rapidities from the eigenvalues of $\mathbf{L}_{22} = -i2\mathbf{H} + \mathbf{M} + \mathbf{M}'$. This leads to the following dispersion relation for rapidies as $\beta(k)$

$$\beta(k) = \frac{g}{4}\left(|1+\delta|^2 + |1-\delta|^2\right) - i|w|\sin\phi_w \sin k + \pm\frac{1}{2}\sqrt{\Lambda}, \tag{37}$$

where

$$\Lambda = i4g\left(|1+\delta|^2 - |1-\delta|^2\right)\mathrm{Im}(\Delta)\sin k - 4\left(|w|\cos\phi_w\cos k + \frac{\mu}{2}\right)^2 - 16|\Delta|^2\sin^2 k \tag{38}$$

$$+i16g\mathrm{Re}(\Delta)\mathrm{Im}(\delta)\sin k + \frac{g^2}{4}\left(|1+\delta|^4 + |1-\delta|^4\right) - \frac{g^2}{2}|1-\delta^2|^2 + 4g^2\mathrm{Im}(\delta)^2. \tag{39}$$

Data availability
Any relevant data are available from the authors upon reasonable request.

Code availability
Any relevant codes are available from the authors upon reasonable request.

Received: 24 April 2022; Accepted: 17 November 2022;
Published online: 07 December 2022

References
1. Valagiannopoulos, C., Sarsen, A. & Alù, A. Angular memory of photonic metasurfaces. *IEEE Trans. Antennas Propag.* **69**, 7720–7728 (2021).
2. Valagiannopoulos, C. Multistability in coupled nonlinear metasurfaces. *IEEE Trans. Antennas Propag.* **70**, 5534–5540 (2022).
3. Ding, D.-S., Busche, H., Shi, B.-S., Guo, G.-C. & Adams, C. S. Phase diagram and self-organizing dynamics in a thermal ensemble of strongly interacting rydberg atoms. *Phys. Rev. X* **10**, 021023 (2020).
4. Ferri, F. et al. Emerging dissipative phases in a superradiant quantum gas with tunable decay. *Phys. Rev. X* **11**, 041046 (2021).
5. Landa, H., Schiró, M. & Misguich, G. Multistability of driven-dissipative quantum spins. *Phys. Rev. Lett.* **124**, 043601 (2020).
6. Chan, C.-K., Lee, T. E. & Gopalakrishnan, S. Limit-cycle phase in driven-dissipative spin systems. *Phys. Rev. A* https://doi.org/10.1103/PhysRevA.91.051601 (2015).
7. Tangpanitanon, J. et al. Hidden order in quantum many-body dynamics of driven-dissipative nonlinear photonic lattices. *Phys. Rev. A* **99**, 043808 (2019).
8. Bácsi, A., Moca, CuuuuPmc, Zaránd, G. & Dóra, B. Vaporization dynamics of a dissipative quantum liquid. *Phys. Rev. Lett.* **125**, 266803 (2020).
9. Letscher, F., Thomas, O., Niederprüm, T., Fleischhauer, M. & Ott, H. Bistability versus metastability in driven dissipative rydberg gases. *Phys. Rev. X* https://doi.org/10.1103/PhysRevX.7.021020 (2017).
10. Mendoza-Arenas, J. J. et al. Beyond mean-field bistability in driven-dissipative lattices: bunching-antibunching transition and quantum simulation. *Phys. Rev. A* **93**, 023821 (2016).
11. Parmee, C. D. & Cooper, N. R. Steady states of a driven dissipative dipolar XXZ chain. *J. Phys. B At. Mol. Optical Phys.* **53**, 135302 (2020).
12. Foss-Feig, M. et al. Emergent equilibrium in many-body optical bistability. *Phys. Rev. A* **95**, 043826 (2017).
13. Baas, A., Karr, J. P., Eleuch, H. & Giacobino, E. Optical bistability in semiconductor microcavities. *Phys. Rev. A* **69**, 023809 (2004).
14. Scarlatella, O., Clerk, A. A., Fazio, R. & Schiró, M. Dynamical mean-field theory for markovian open quantum many-body systems. *Phys. Rev. X* **11**, 031018 (2021).
15. Patra, A., Altshuler, B. L. & Yuzbashyan, E. A. Driven-dissipative dynamics of atomic ensembles in a resonant cavity: Nonequilibrium phase diagram and periodically modulated superradiance. *Phys. Rev. A* **99**, 033802 (2019).
16. Sciolla, B., Poletti, D. & Kollath, C. Two-time correlations probing the dynamics of dissipative many-body quantum systems: aging and fast relaxation. *Phys. Rev. Lett.* **114**, 170401 (2015).
17. Müller, T., Gievers, M., Fröml, H., Diehl, S. & Chiocchetta, A. Shape effects of localized losses in quantum wires: Dissipative resonances and nonequilibrium universality. *Phys. Rev. B* https://doi.org/10.1103/PhysRevB.104.155431 (2021).
18. Kunimi, M. & Danshita, I. Nonequilibrium steady states of bose-einstein condensates with a local particle loss in double potential barriers. *Phys. Rev. A* **100**, 063617 (2019).
19. Piazza, F. & Ritsch, H. Self-ordered limit cycles, chaos, and phase slippage with a superfluid inside an optical resonator. *Phys. Rev. Lett.* **115**, 163601 (2015).
20. Mivehvar, F., Piazza, F., Donner, T. & Ritsch, H. Cavity qed with quantum gases: new paradigms in many-body physics. *Adv. Phys.* **70**, 1 (2021).
21. Mc Keever, C. & Szymańska, M. H. Stable ipepo tensor-network algorithm for dynamics of two-dimensional open quantum lattice models. *Phys. Rev. X* **11**, 021035 (2021).
22. Lambert, M. R., Tsai, S.-W. & Kelly, S. P. Quantum memory at an eigenstate phase transition in a weakly chaotic model. *Phys. Rev. A* **106**, 012206 (2022).
23. Aldana, S., Bruder, C. & Nunnenkamp, A. Equivalence between an optomechanical system and a kerr medium. *Phys. Rev. A* **88**, 043826 (2013).
24. Pizzi, A., Nunnenkamp, A. & Knolle, J. Bistability and time crystals in long-ranged directed percolation. *Nat. Commun.* https://doi.org/10.1038/s41467-021-21259-4 (2021).
25. Carollo, F. & Lesanovsky, I. Exact solution of a boundary time-crystal phase transition: time-translation symmetry breaking and non-markovian dynamics of correlations. *Phys. Rev. A* **105**, L040202 (2022).
26. Kazemi, J. & Weimer, H. Genuine bistability in open quantum many-body systems. Preprint at https://arxiv.org/abs/2111.05352 (2021).
27. Owen, E. T., Jin, J., Rossini, D., Fazio, R. & Hartmann, M. J. Quantum correlations and limit cycles in the driven-dissipative heisenberg lattice. *N. J. Phys.* **20**, 045004 (2018).
28. Roberts, D. & Clerk, A. A. Driven-dissipative quantum kerr resonators: new exact solutions, photon blockade and quantum bistability. *Phys. Rev. X* **10**, 021022 (2020).
29. de Melo, N. R. et al. Intrinsic optical bistability in a strongly driven rydberg ensemble. *Phys. Rev. A* **93**, 063863 (2016).
30. Cabot, A., Giorgi, G. L. & Zambrini, R. Metastable quantum entrainment. *N. J. Phys.* **23**, 103017 (2021).
31. Buča, B., Tindall, J. & Jaksch, D. Non-stationary coherent quantum many-body dynamics through dissipation. *Nat. Commun.* **10**, 1730 (2019).
32. Keßler, H. et al. Observation of a dissipative time crystal. *Phys. Rev. Lett.* **127**, 043602 (2021).

33. Kongkhambut, P. et al. Observation of a continuous time crystal. *Science* **377**, 670–673 (2022).
34. Seibold, K., Rota, R. & Savona, V. Dissipative time crystal in an asymmetric nonlinear photonic dimer. *Phys. Rev. A* **101**, 033839 (2020).
35. Tucker, K. et al. Shattered time: can a dissipative time crystal survive many-body correlations? *N. J. Phys.* **20**, 123003 (2018).
36. Seibold, K., Rota, R., Minganti, F. & Savona, V. Quantum dynamics of dissipative kerr solitons. *Phys. Rev. A* **105**, 053530 (2022).
37. Buča, B. & Jaksch, D. Dissipation induced nonstationarity in a quantum gas. *Phys. Rev. Lett.* **123**, 260401 (2019).
38. Keßler, H., Cosme, J. G., Georges, C., Mathey, L. & Hemmerich, A. From a continuous to a discrete time crystal in a dissipative atom-cavity system. *N. J. Phys.* **22**, 085002 (2020).
39. Minganti, F., Arkhipov, I. I., Miranowicz, A. & Nori, F. Correspondence between dissipative phase transitions of light and time crystals. Preprint at https://arxiv.org/abs/2008.08075 (2020).
40. Dogra, N. et al. Dissipation-induced structural instability and chiral dynamics in a quantum gas. *Science* **366**, 1496–1499 (2019).
41. Zupancic, P. et al. *p*-band induced self-organization and dynamics with repulsively driven ultracold atoms in an optical cavity. *Phys. Rev. Lett.* **123**, 233601 (2019).
42. Booker, C., Buča, B. & Jaksch, D. Non-stationarity and dissipative time crystals: Spectral properties and finite-size effects. *N. J. Phys*. https://iopscience.iop.org/article/10.1088/1367-2630/ababc4 (2020).
43. Chinzei, K. & Ikeda, T. N. Time crystals protected by floquet dynamical symmetry in hubbard models. *Phys. Rev. Lett.* **125**, 060601 (2020).
44. Chinzei, K. & Ikeda, T. N. Criticality and rigidity of dissipative discrete time crystals in solids. *Phys. Rev. Res.* **4**, 023025 (2022).
45. Sarkar, S. & Dubi, Y. Signatures of discrete time-crystallinity in transport through quantum dot arrays. *Commun. Phys.* **5**, 155 (2022).
46. Taheri, H., Matsko, A. B., Maleki, L. & Sacha, K. All-optical dissipative discrete time crystals. *Nat. Commun.* **13**, 848 (2022).
47. Iemini, F. et al. Boundary time crystals. *Phys. Rev. Lett.* **121**, 035301 (2018).
48. Piccitto, G., Wauters, M., Nori, F. & Shammah, N. Symmetries and conserved quantities of boundary time crystals in generalized spin models. *Phys. Rev. B* **104**, 014307 (2021).
49. Marcuzzi, M., Levi, E., Diehl, S., Garrahan, J. P. & Lesanovsky, I. Universal nonequilibrium properties of dissipative rydberg gases. *Phys. Rev. Lett.* **113**, 210401 (2014).
50. Lourenço, A. C., dos Prazeres, L. F., Maciel, T. O., Iemini, F. & Duzzioni, E. I. Genuine multipartite correlations in a boundary time crystal. *Phys. Rev. B* **105**, 134422 (2022).
51. Hajdušek, M., Solanki, P., Fazio, R. & Vinjanampathy, S. Seeding crystallization in time. *Phys. Rev. Lett.* **128**, 080603 (2022).
52. Gong, Z., Hamazaki, R. & Ueda, M. Discrete time-crystalline order in cavity and circuit qed systems. *Phys. Rev. Lett.* https://doi.org/10.1103/PhysRevLett.120.040404 (2018).
53. Liu, T., Zhang, Y.-R., Xu, K., Cui, J. & Fan, H. Discrete time crystal in a driven-dissipative bose-hubbard model with two-photon processes. *Phys. Rev. A* **105**, 013710 (2022).
54. Lledó, C., Mavrogordatos, T. K. & Szymańska, M. Driven bose-hubbard dimer under nonlocal dissipation: A bistable time crystal. *Phys. Rev. B* **100**, 054303 (2019).
55. Natsheh, M., Gambassi, A. & Mitra, A. Critical properties of the prethermal floquet time crystal. *Phys. Rev. B* **103**, 224311 (2021).
56. Lazarides, A., Roy, S., Piazza, F. & Moessner, R. Time crystallinity in dissipative floquet systems. *Phys. Rev. Res.* https://doi.org/10.1103/PhysRevResearch.2.022002 (2020).
57. McGinley, M., Roy, S. & Parameswaran, S. A. Absolutely stable spatiotemporal order in noisy quantum systems. *Phys. Rev. Lett.* **129**, 090404 (2022).
58. Carollo, F., Brandner, K. & Lesanovsky, I. Nonequilibrium many-body quantum engine driven by time-translation symmetry breaking. *Phys. Rev. Lett.* **125**, 240602 (2020).
59. Ney, P.-M., Notarnicola, S., Montangero, S. & Morigi, G. Entanglement in the quantum game of life. *Phys. Rev. A* https://doi.org/10.1103/PhysRevA.105.012416 (2022).
60. Mendoza-Arenas, J. J. & Buča, B. Self-induced entanglement resonance in a disordered bose-fermi mixture. https://arxiv.org/abs/2106.06277 (2021).
61. Yuan, D., Zhang, S.-Y., Wang, Y., Duan, L. M. & Deng, D.-L. Quantum information scrambling in quantum many-body scarred systems. *Phys. Rev. Res.* **4**, 023095 (2022).
62. Sánchez Muñoz, C. et al. Symmetries and conservation laws in quantum trajectories: dissipative freezing. *Phys. Rev. A* **100**, 042113 (2019).
63. Turner, C. J., Michailidis, A. A., Abanin, D. A., Serbyn, M. & Papić, Z. Weak ergodicity breaking from quantum many-body scars. *Nat. Phys.* **14**, 745–749 (2018).
64. Choi, S. et al. Emergent SU(2) dynamics and perfect quantum many-body scars. *Phys. Rev. Lett.* **122**, 220603 (2019).
65. Moudgalya, S., Regnault, N. & Bernevig, B. A. Eta-pairing in hubbard models: from spectrum generating algebras to quantum many-body scars. *Phys. Rev. B* **102**, 085140 (2020).
66. Bull, K., Desaules, J.-Y. & Papić, Z. Quantum scars as embeddings of weakly broken lie algebra representations. *Phys. Rev. B* **101**, 165139 (2020).
67. Mark, D. K. & Motrunich, O. I. Eta-pairing states as true scars in an extended Hubbard Model. *Phys. Rev. B* **102**, 075132 (2020).
68. Pakrouski, K., Pallegar, P. N., Popov, F. K. & Klebanov, I. R. Many body scars as a group invariant sector of hilbert space. *Phys. Rev. Lett.* **125**, 230602 (2020).
69. Serbyn, M., Abanin, D. A. & Papić, Z. Quantum many-body scars and weak breaking of ergodicity. *Nat. Phys.* **17**, 675–685 (2021).
70. Pakrouski, K., Pallegar, P. N., Popov, F. K. & Klebanov, I. R. Group theoretic approach to many-body scar states in fermionic lattice models. *Phys. Rev. Res.* **3**, 043156 (2021).
71. Michailidis, A. A., Turner, C. J., Papić, Z., Abanin, D. A. & Serbyn, M. Stabilizing two-dimensional quantum scars by deformation and synchronization. *Phys. Rev. Res.* **2**, 022065 (2020).
72. You, W.-L. et al. Quantum many-body scars in spin-1 kitaev chains. *Phys. Rev. Res.* https://doi.org/10.1103/PhysRevResearch.4.013103 (2022).
73. Castro-Alvaredo, O. A., Lencsés, M., Szécsényi, I. M. & Viti, J. Entanglement oscillations near a quantum critical point. *Phys. Rev. Lett.* **124**, 230601 (2020).
74. Castro-Alvaredo, O. A., Lencsés, M., Szécsényi, I. M. & Viti, J. Entanglement dynamics after a quench in ising field theory: a branch point twist field approach. *J. High Energy Phys.* https://doi.org/10.1007/JHEP12(2019)079 (2019).
75. Tindall, J., Buča, B., Coulthard, J. R. & Jaksch, D. Heating-induced long-range η pairing in the hubbard model. *Phys. Rev. Lett.* **123**, 030603 (2019).
76. Sala, P., Lehmann, J., Rakovszky, T. & Pollmann, F. Dynamics in systems with modulated symmetries. https://arxiv.org/abs/2110.08302 (2021).
77. Barut, A., Bohm, A. & Ne'eman, Y. *Dynamical Groups and Spectrum Generating Algebras* (World Scientific Publishing Company, 1988).
78. Medenjak, M., Buča, B. & Jaksch, D. Isolated Heisenberg magnet as a quantum time crystal. *Phys. Rev. B* **102**, 041117 (2020).
79. Moudgalya, S., Bernevig, B. A. & Regnault, N. Quantum many-body scars and hilbert space fragmentation: a review of exact results. *Rep. Prog. Phys.* **85**, 086501 (2022).
80. Fagotti, M. Global quenches after localised perturbations. *Phys. Rev. Lett.* **128**, 110602 (2022).
81. Medenjak, M., Prosen, T. & Zadnik, L. Rigorous bounds on dynamical response functions and time-translation symmetry breaking. *SciPost Phys.* **9**, 003 (2020).
82. Buča, B. & Prosen, T. A note on symmetry reductions of the lindblad equation: transport in constrained open spin chains. *N. J. Phys.* **14**, 073007 (2012).
83. Albert, V. V. & Jiang, L. Symmetries and conserved quantities in lindblad master equations. *Phys. Rev. A* **89**, 022118 (2014).
84. Mirrahimi, M. et al. Dynamically protected cat-qubits: a new paradigm for universal quantum computation. *N. J. Phys.* **16**, 045014 (2014).
85. Albert, V. V. Lindbladians with multiple steady states: theory and applications. https://arxiv.org/abs/1802.00010 (2018).
86. Halati, C.-M., Sheikhan, A. & Kollath, C. Breaking strong symmetries in dissipative quantum systems: Bosonic atoms coupled to a cavity. *Phys. Rev. Res.* **4**, L012015 (2022).
87. Lieu, S. et al. Symmetry breaking and error correction in open quantum systems. *Phys. Rev. Lett.* **125**, 240405 (2020).
88. Flynn, V. P., Cobanera, E. & Viola, L. Topology by dissipation: Majorana bosons in metastable quadratic markovian dynamics. *Phys. Rev. Lett.* **127**, 245701 (2021).
89. McDonald, A. & Clerk, A. A. Exact solutions of interacting dissipative systems via weak symmetries. *Phys. Rev. Lett.* **128**, 033602 (2022).
90. van Caspel, M. & Gritsev, V. Symmetry-protected coherent relaxation of open quantum systems. *Phys. Rev. A* https://doi.org/10.1103/PhysRevA.97.052106 (2018).
91. Nigro, D. Complexity of the steady state of weakly symmetric open quantum lattices. *Phys. Rev. A* https://doi.org/10.1103/PhysRevA.101.022109 (2020).
92. Dutta, S., Kuhr, S. & Cooper, N. R. Generating symmetry-protected long-range entanglement in many-body systems. https://arxiv.org/abs/2201.10564 (2022).
93. Manzano, D., Martínez-García, M. A. & Hurtado, P. I. Coupled activity-current fluctuations in open quantum systems under strong symmetries. *N. J. Phys.* **23**, 073044 (2021).
94. Nakagawa, M., Tsuji, N., Kawakami, N. & Ueda, M. η pairing of light-emitting fermions: nonequilibrium pairing mechanism at high temperatures. https://arxiv.org/abs/2103.13624 (2021).
95. Seetharam, K., Lerose, A., Fazio, R. & Marino, J. Correlation engineering via nonlocal dissipation. *Phys. Rev. Res.* **4**, 013089 (2022).

96. Marino, J. Universality class of ising critical states with long-range losses. *Phys. Rev. Lett.* **129**, 050603 (2022).
97. Kitaev, A. Fault-tolerant quantum computation by anyons. *Ann. Phys.* **303**, 2–30 (2003).
98. Chiu, C.-K., Pikulin, D. I. & Franz, M. Strongly interacting majorana fermions. *Phys. Rev. B* **91**, 165402 (2015).
99. Mahyaeh, I. & Ardonne, E. Zero modes of the kitaev chain with phase-gradients and longer range couplings. *J. Phys. Commun.* **2**, 045010 (2018).
100. Hung, J. S. C. et al. Quantum simulation of the bosonic creutz ladder with a parametric cavity. *Phys. Rev. Lett.* **127**, 100503 (2021).
101. Fendley, P. Parafermionic edge zero modes inzn-invariant spin chains. *J. Stat. Mech. Theory Exp.* **2012**, P11020 (2012).
102. Shibata, N., Yoshioka, N. & Katsura, H. Onsager's scars in disordered spin chains. *Phys. Rev. Lett.* **124**, 180604 (2020).
103. Chitov, G. Y. Local and nonlocal order parameters in the kitaev chain. *Phys. Rev. B* **97**, 085131 (2018).
104. van Caspel, M., Arze, S. E. T. & Castillo, I. P. Dynamical signatures of topological order in the driven-dissipative Kitaev chain. *SciPost Phys.* **6**, 26 (2019).
105. Diehl, S., Rico, E., Baranov, M. A. & Zoller, P. Topology by dissipation in atomic quantum wires. *Nat. Phys.* https://doi.org/10.1038/nphys2106 (2011).
106. Buca, B., Booker, C. & Jaksch, D. Algebraic theory of quantum synchronization and limit cycles under dissipation. *SciPost Phys* **12**, 097 (2022).
107. Muñoz, C. S. et al. Non-stationary dynamics and dissipative freezing in squeezed superradiance. https://arxiv.org/abs/1903.05080 (2019).
108. Barthel, T. & Schollwöck, U. Dephasing and the steady state in quantum many-particle systems. *Phys. Rev. Lett.* **100**, 100601 (2008).
109. Jordan, P. & Wigner, E. Über das paulische Äquivalenzverbot. *Zeitschrift für Physik* https://doi.org/10.1007/BF01331938 (1928).
110. Doyon, B. Hydrodynamic projections and the emergence of linearised euler equations in one-dimensional isolated systems. *Commun. Math. Phys.* **391**, 293 (2022).
111. Ampelogiannis, D. & Doyon, B. Almost everywhere ergodicity in quantum lattice models. https://arxiv.org/abs/2112.12730 (2021).
112. Ampelogiannis, D. & Doyon, B. Ergodicity and hydrodynamic projections in quantum spin lattices at all frequencies and wavelengths. https://arxiv.org/abs/2112.12747 (2021).
113. Gunawardana, T. M. & Buča, B. Dynamical l-bits and persistent oscillations in Stark many-body localization. *Phys. Rev. B* **106**, L161111 (2022).
114. Buča, B. Out-of-Time-Ordered Crystals and Fragmentation. *Phys. Rev. Lett.* **128**, 100601 (2022).
115. Buca, B. et al. Quantum many-body attractors. https://arxiv.org/abs/2008.11166 (2020).
116. Ilievski, E. & Prosen, T. Thermodyamic bounds on drude weights in terms of almost-conserved quantities. *Commun. Math. Phys.* **318**, 809–830 (2012).
117. Zhang, Z., Tindall, J., Mur-Petit, J., Jaksch, D. & Buča, B. Stationary state degeneracy of open quantum systems with non-abelian symmetries. *J. Phys. A Math. Theor.* **53**, 215304 (2020).
118. Macieszczak, K., Guţă, M., Lesanovsky, I. & Garrahan, J. P. Towards a theory of metastability in open quantum dynamics. *Phys. Rev. Lett.* **116**, 240404 (2016).
119. Macieszczak, K. Operational approach to metastability. https://arxiv.org/abs/2104.05095 (2021).
120. Macieszczak, K., Rose, D. C., Lesanovsky, I. & Garrahan, J. P. Theory of classical metastability in open quantum systems. *Phys. Rev. Res.* **3**, 033047 (2021).
121. Cai, Z. & Barthel, T. Algebraic versus exponential decoherence in dissipative many-particle systems. *Phys. Rev. Lett.* **111**, 150403 (2013).
122. Žnidarič, M. Relaxation times of dissipative many-body quantum systems. *Phys. Rev. E* **92**, 042143 (2015).
123. Medvedyeva, M. V. & Kehrein, S. Power-law approach to steady state in open lattices of noninteracting electrons. *Phys. Rev. B* **90**, 205410 (2014).
124. Prosen, T. Third quantization: a general method to solve master equations for quadratic open fermi systems. *N. J. Phys.* **10**, 043026 (2008).
125. Bakker, L. R., Yashin, V. I., Kurlov, D. V., Fedorov, A. K. & Gritsev, V. Lie-algebraic approach to one-dimensional translationally invariant free-fermionic dissipative systems. *Phys. Rev. A* **102**, 052220 (2020).
126. Tindall, J., Sánchez Muñoz, C., Buča, B. & Jaksch, D. Quantum synchronisation enabled by dynamical symmetries and dissipation. *N. J. Phys.* **22**, 013026 (2020).
127. Roulet, A. & Bruder, C. Quantum synchronization and entanglement generation. *Phys. Rev. Lett.* **121**, 063601 (2018).
128. Solanki, P., Jaseem, N., Hajdušek, M. & Vinjanampathy, S. Role of coherence and degeneracies in quantum synchronisation. *Phys. Rev. A* **105**, L020401 (2022).

Acknowledgements

H.A. acknowledges the Purdue University Startup fund. B.B. acknowledges funding from the EPSRC programme grant EP/P009565/1, the EPSRC National Quantum Technology Hub in Networked Quantum Information Technology (EP/M013243/1), and the VILLUM FONDEN by Research Grant No. 42085.

Author contributions

H.A. did the calculations for the quadratic model, numerical simulations, and wrote the majority of the text. B.B. proposed, designed, and led the research and calculated the dynamical symmetries. All authors contributed to discussions.

Competing interests

The authors declare no competing interests.

Additional information

Supplementary information The online version contains supplementary material available at https://doi.org/10.1038/s42005-022-01090-z.

Correspondence and requests for materials should be addressed to Berislav Buča.

Peer review information *Communications Physics* thanks Maurizio Fagotti, Cristóbal Lledó and the other, anonymous, reviewer(s) for their contribution to the peer review of this work. Peer reviewer reports are available.

Reprints and permission information is available at http://www.nature.com/reprints

Publisher's note Springer Nature remains neutral with regard to jurisdictional claims in published maps and institutional affiliations.